Published in final edited form as:
Nat Genet. 2010 October ; 42(10): 910–914. doi:10.1038/ng.665.

Keratin 17 promotes epithelial proliferation and tumor growth by polarizing the immune response in skin

Daryle DePianto[1], **Michelle Kerns**[1], **Andrzej A. Dlugosz**[2,3], and **Pierre A. Coulombe**[1,4,5,#]

[1]Dept. of Biochemistry and Molecular Biology, Bloomberg School of Public Health, Johns Hopkins University, Baltimore, MD, USA

[2]Department of Dermatology, University of Michigan School of Medicine, Ann Arbor, MI, USA

[3]Department of Cell and Developmental Biology, University of Michigan School of Medicine, Ann Arbor, MI, USA

[4]Department of Biological Chemistry, Johns Hopkins University, Baltimore, MD, USA

[5]Department Dermatology, School of Medicine, Johns Hopkins University, Baltimore, MD, USA

Abstract

Basaloid skin tumors, including basal cell carcinoma (BCC) and basaloid follicular hamartoma (BFH), are associated with aberrant Hedgehog (Hh) signaling1 and, in the case of BCC, an expanding set of genetic variants including keratin 5 (K5)2, an intermediate filament-forming protein. We show that genetic ablation of keratin 17 (K17) protein, which is induced in basaloid skin tumors3,4 and co-polymerizes with K5 in vivo5, delays BFH tumor initiation and growth in mice with constitutive Hh signaling in epidermis6,7. The delay is preceded by reduced inflammation and a polarization of inflammatory cytokines from a Th1/Th17- to a Th2-dominated profile. Absence of K17 also attenuates hyperplasia and inflammation in a model of acute dermatitis. Re-expression of K17 in *Gli2*^{tg} *K17*$^{-/-}$ keratinocytes induces select Th1 chemokines with established roles in BCC. Our findings establish a novel immunomodulatory role for K17 in Hh-driven basaloid skin tumors that could impact additional tumor settings, psoriasis, and wound repair.

[#]To whom correspondence should be addressed: Dr. Pierre A. Coulombe, Dept. of Biochemistry and Molecular Biology, Johns Hopkins Bloomberg School of Public Health, 615 N. Wolfe St., Room W8041, Baltimore, MD, USA. Tel: 410-955-3671, coulombe@jhsph.edu.

Note: Supplementary information is available on the Nature Genetics website.

AUTHOR CONTRIBUTIONS

D.D. conceived and led the execution of all experiments, and participated in the interpretation of the results and manuscript production.

M.K. contributed expertise about inflammatory and immune cytokines, and assisted D.D. in the execution and interpretation of many experiments.

A.A.D. contributed expertise on mouse skin tumor models and skin tumor histology, and participated in manuscript production.

P.A.C. conceived the experiments along with D.D. and participated in the interpretation of the results and manuscript production.

COMPETING FINANCIAL INTERESTS

The authors declare no competing financial interests.

Main Text

Gli2^{tg} mice, in which the bovine *K5* promoter drives the constitutive expression of mouse Gli26, develop BCC and BFH6,7, which are both linked to deregulated Hh signaling in humans7,8. *Gli2*^{tg} mice show a reproducible pattern of lesions on the ear that successively involves hyper-keratosis (flaking), thickening and hyperpigmentation (Supplemental Fig. 1a). Mice were scored as positive for the onset of lesions upon the first sign of macroscopic hyperkeratosis in ear tissue. Histologically, the lesions present between P80 and P120 resemble BFH as described 7,8. By P180, larger, nodular, BCC-like tumors frequently occur deeper in the dermis (Supplemental Fig. 1a). Male *Gli2*^{tg} mice consistently develop lesions earlier than females (Supplemental Fig. 1b). Induction of *K17*, a Gli target gene9, is the main alteration in keratin expression prior to onset of lesions in *Gli2*^{tg} epidermis (Supplemental Fig. 1c).

Gli2^{tg} and *K17*$^{-/-}$ mice6,10 were interbred so as to assess the impact of *K17* loss on genesis of BFH-like tumors. Appearance and progression of hamartoma-like lesions were captured from P30 to P125. At P80, epithelial lesions are clearly less pronounced in *Gli2*^{tg}*/K17*$^{-/-}$ than in *Gli2*^{tg} ear tissue (Fig. 1a; male data shown). In male *Gli2*^{tg} and *Gli2*^{tg}*/K17*$^{-/-}$ mice the average onset of lesions is 65±2 days (n=32) and 91±2 days (n=31; $p< 0.01$), respectively. In females, onset is at 80±5 days (Gli2^{tg}; n=22) vs. 101±2 days (Gli2^{tg}/K17$^{-/-}$; n=21; $p< 0.01$)(Fig. 1b; Supplemental Fig. 2a). *Gli2*^{tg} mice lacking K1411 do not display such a delay (Fig. 1c), establishing specificity. Gli2 transgene expression is similar in both genotypes (Fig. 1d). Loss of *K17* does not impact Gli2 subcellular localization or hedgehog signaling (Supplemental Fig. 2, b–d). Therefore, the absence of K17 causes a delay in the inception of BFH-like skin tumors in *Gli2*^{tg} mice.

Histological anomalies common to Hh pathway-activated mouse skin7 were scored in *Gli2*^{tg} and *Gli2*^{tg}*/K17*$^{-/-}$ ear tissue (Supplementary Fig. 3a). Such anomalies, absent in wildtype and *K17*$^{-/-}$ mouse ears (Supplementary Fig. 3b), are prominent in *Gli2*^{tg} ear but markedly reduced in *Gli2*^{tg}*/K17*$^{-/-}$ ear (Supplementary Fig. 3c). Overall tissue thickness and penetration of epithelial downgrowths are also reduced in *Gli2*^{tg}*/K17*$^{-/-}$ ear tissue (Supplementary Fig. 3d,e). K17, K5, and K14 are uniformly distributed in the lesional epithelium (Supplemental Fig. 3f). Co-assembly of K5 and K17 in *Gli2*^{tg} lesional epithelium is conveyed by their co-localization and co-immunoprecipitation (Supplemental Fig. 3g,h). The wound-inducible K6α, K6β and K16, absent in intact epidermis, are induced in the upper layers of thickened *Gli2*^{tg} epidermis, preferentially, but are markedly reduced in *Gli2*^{tg}*/K17*$^{-/-}$ skin (Supplemental Fig. 3f,i).

Reduced proliferation, rather than increased cell death, is a key contributor to delayed tumor onset in *Gli2*^{tg}*/K17*$^{-/-}$ skin. Relative to *Gli2*^{tg}, indeed, the frequency of mitotically-active cells is depressed by > 3-fold in *Gli2*^{tg}*/K17*$^{-/-}$ ear epithelium (Fig. 1e–g). In contrast, TUNEL-positive, apoptotic cells are restricted to the upper epidermis of lesional skin and show similar density in both genotypes (Fig. 1h).

Inflammation has emerged as a driver of angiogenesis and tumor growth12 and coincides with K17 induction and loss of barrier function in several skin diseases13,14.

Immunoreactivity for markers of innate immune cells (CD11b), T cells (Thy-1), and phagocytes (iNOS) are enhanced in *Gli2*^{tg} compared to *Gli2*^{tg}*/K17*$^{-/-}$ ear skin of p80 male mice (Fig. 2a). PECAM staining is also decreased in *Gli2*^{tg}*/K17*$^{-/-}$ ear skin (Fig. 2a), reflecting decreased angiogenesis. Myeloperoxidase (MPO) enzymatic activity, inherent to neutrophils15, is increased 17.4 ± 0.5 fold in P80 male *Gli2*^{tg} ear tissue but only 5.8 ± 0.1 fold in *Gli2*^{tg}*/K17*$^{-/-}$ males (data normalized to P80 female *Gli2*^{tg} ear; Fig. 2b). Female *Gli2*^{tg}*/K17*$^{-/-}$ mice also show a reduced level of MPO activity at P80, being at 0.75 fold of that seen in *Gli2*^{tg} controls (Fig. 2b). Skin barrier integrity, assessed via a whole-mount dye penetration assay16, is intact as expected in P70 wildtype ear skin (Fig. 2c). In contrast, a sizable portion of the ear is dye-permeable in P70 *Gli2*^{tg} mice (Fig. 2c); again, this readout is markedly decreased in *Gli2*^{tg}*/K17*$^{-/-}$ mice (Fig. 2c).

At P40, i.e., prior to onset of histological anomalies (Fig. 2d), MPO activity is 5.9±1.9 fold greater in male *Gli2*^{tg} mice relative to females, substantiating the gender bias in this model. MPO activity is lower in P40 male *Gli2*^{tg}*/K17*$^{-/-}$ mice (0.55 ± 0.20 relative to female *Gli2*^{tg} mice; Fig. 2e). While epidermal thickness is the same (Fig. 2d), mitotic activity is higher in *Gli2*^{tg} vs. *Gli2*^{tg}*/K17*$^{-/-}$ epidermis at P40 (0.52 ± 0.01 vs. 0.14 ± 0.02 BrdU labeled cells/mm of epidermis) (Fig. 2f) and skin tissue is infiltrated with various types of leukocytes. Barrier integrity is mildy compromised in P40 *Gli2*^{tg} ear skin, is again better preserved in *Gli2*^{tg}*/K17*$^{-/-}$ mice (Supplemental Fig. 4a). Thus, the marked reductions in inflammation and hyperplasia that define *Gli2*^{tg}*/K17*$^{-/-}$ ear skin occur as early as P40, ahead of progression to overt tumorigenesis in the *Gli2*^{tg} model.

Expression of inflammatory cytokines and chemokines was examined via qRT-PCR in ear tissue at P40 and P80. The findings are stratified according to specific classes of T-helper cytokines: Th1 (cellular immunity; generally “pro-inflammatory”), Th2 (humoral immunity; “anti-inflammatory”), and Th17 (anti-microbial immunity at epithelial barriers)17,18. Th1 and Th17 hyperactivity occur in psoriasis19. Absence of K17 in *Gli2*^{tg} skin correlates with a marked reduction in Th1- and Th17-related markers and induction of Th2-related markers (Table 1), many of which are prominently expressed by skin keratinocytes themselves. Expression of IL-1β, a keratinocyte mitogen20, is ~10 fold higher in *Gli2*^{tg} compared to *Gli2*^{tg}*/K17*$^{-/-}$ skin (Table 1). Immunostaining shows that IL-1β epitopes are strongly expressed in the skin epithelium (Fig. 2g). Spp1 (osteopontin), which acts to bias immune responses toward Th121, is reduced by ~15 fold and IL-6, associated with the acute phase response and upregulated in human BCC22, is lowered ~17 fold in *Gli2*^{tg}*/K17*$^{-/-}$ skin (Table1). The matrix metalloproteases MMP3, MMP9 and MMP13, whose expression is enhanced in BCC23, are downregulated in *Gli2*^{tg}*/K17*$^{-/-}$ ear tissue. Classical Th2 type cytokines primarily secreted by T-cells, e.g., IL-4 and IL-10, are modestly altered whereas Ccl24 and Ccr4, expressed by skin keratinocytes24, are respectively ~9 and ~3 fold higher in *Gli2*^{tg}*/K17*$^{-/-}$ ear tissue (Table 1). The expression of many of these cytokines and chemokines is already altered by P40. IL1β and Cxcl5 expression is enhanced in the presence of K17, while the Th2 markers IL20 and IL4 are enhanced in its absence (Table 1). Thus, the immunomodulatory influence of K17 is first manifested at an early stage in this model.

Topical application of the phorbol ester, 12-O-tetradecanoylphorbol-13-acetate (TPA)25, to ear skin induces acute inflammation and epidermal proliferation (Fig. 3a,b), providing a tumor-free, dermatitis-like setting in which to assess the impact of *K17* loss. The latter curtails hyperplasia-driven epidermal thickening (*wt* ear tissue: 34.1±2.3 μm in TPA- vs. 10.4±0.3 μm in vehicle-treated; $K17^{-/-}$ ear tissue: 18.7± 0.8 μm in TPA- vs. 10.6±0.8 μm in vehicle-treated; Fig. 3a,b). Markers related to compromised skin barrier function (S100A826, thymic stromal lymphoprotein (TSLP)14, β-defensin 27) show elevated mRNA levels in TPA-treated wildtype skin (Fig. 3c). TSLP and β–defensin are markedly attenuated in $K17^{-/-}$ skin (Fig. 3c), suggesting better retention of barrier function. A partial shift toward a Th2-dominated cytokine profile is seen in TPA-treated $K17^{-/-}$ skin, though the magnitude of the changes is less than in $Gli2^{tg}$ skin. The Th1 chemokines Cxcl5, Ccl3 and IL-1β are reduced 2.4-, 3.0- and 1.7-fold, respectively, and the Th2 cytokine IL-20 is 7.1 fold higher in TPA-treated $K17^{-/-}$ skin relative to control (Table 2). Thus, the *K17* status exerts a similar immunomodulatory influence in acute dermatitis.

Skin keratinocytes from $Gli2^{tg}$ and $Gli2^{tg}/K17^{-/-}$ newborn mice were seeded for primary culture (48h), and treated with TPA (12h) to assess whether key changes in cytokine/chemokine expression are keratinocyte-autonomous. Under basal conditions, $Gli2^{tg}$ and $Gli2^{tg}/K17^{-/-}$ cells show rates of proliferation similar to *wt* and $K17^{-/-}$ ones. TPA induces a two-fold enhancement in $Gli2^{tg}$ keratinocyte proliferation by 12h, whereas $Gli2^{tg}/K17^{-/-}$ cells are unchanged (Supplemental Fig. 4b,c). Again, key chemokines are differentially expressed depending on *K17* status. Levels of Cxcl11, Cxcl5, CxCl9 and Cxcl10 mRNAs, among others, are significantly lower in TPA-treated $Gli2^{tg}/K17^{-/-}$ keratinocytes (Fig. 3d and Supplemental Fig. 4d). These chemokines promote keratinocyte proliferation in skin tumors, and show a tight spatial correlation with K17 expression28,29. Re-expression of K17 into TPA-treated $Gli2^{tg}/K17^{-/-}$ keratinocytes markedly elevates the levels of Cxcl5, CxCl9, and CxCl11 mRNAs, relative to mock-transfected cells (Fig. 3d; Supplemental Fig. 4d). Thus, K17 impacts the TPA-induced expression of select chemokines relevant to BCC pathogenesis in both adult epidermis in situ and isolated newborn keratinocytes in culture, suggesting that the mechanism(s) involved are in part cell-autonomous.

Several NF-kB target genes show a modest but consistent reduction in their expression in $Gli2^{tg}/K17^{-/-}$ relative to $Gli2^{tg}$ keratinocytes in TPA-treated cultures (Supplemental Figure 5a). This is consistent with the prominent role of NF-κB in skin inflammatory conditions 30 and, in particular, with its impact on Cxcl5, CxCl9, and CxCl11 expression31–33. Similar analyses of P80 whole ear skin tissue revealed no difference between the genotypes, likely reflecting the large complexity of these lesions in situ and the occurrence of secondary or compensatory changes (Supplemental Figure 5, b–c). Besides, K17 has been shown to promote anagen growth during hair follicle cycling34 and stimulates protein synthesis during tissue repair35. The phenotype reported here cannot be correlated to obvious alterations in these roles, again as inferred from analyses of skin tissue sections (data not shown) or extracts (Supplemental Fig. 5, b–d).

K17 is ectopically expressed in numerous settings associated with robust inflammation including cutaneous wounds, various carcinomas, psoriasis, and virus-induced warts10. High levels of K17 expression correlate with a poor prognosis in breast36 and pancreatic37 cancers – whether this phenomenon is related to altered inflammatory signatures represents an issue of interest. There exists a correlation between Th1 hyperactivity and K17 expression in psoriatic plaques19; plaque resolution coincides with a shift to a Th2 response and loss of K17 expression. We posit that the presence of K17 in epidermis (and related epithelia) promotes hyperplasia in BCC-like tumors (this study) and likely in additional tumors and inflammatory disease settings in part through its ability to promote a specific type of inflammatory response. Normal contexts in which prominent K17 expression is not correlated to local inflammation (e.g., hair follicles) may benefit from an immune-privileged status38 or reflect its regulation via post-translational modifications or interaction with other proteins34,35. A role for K17 as an immunomodulator, whether direct or indirect, provides a novel way of conceiving how SNPs affecting *K5* influence the risk of developing BCC 2, and makes these keratins potentially attractive target for novel therapies aimed at curtailing conditions driven by or linked to chronic inflammation.

METHODS

Methods and any associated references are available in the online version of the paper at http://www.nature.com/naturegenetics/.

Supplementary Material

Refer to Web version on PubMed Central for supplementary material.

ACKNOWLEDGMENTS

The authors thank Minerva Han for technical support. These studies were supported in part by grants CA123530 and AR44232 to P.A.C., fellowship grant F32 CA110618 to D.D., and grant CA087837 to A.A.D., all from the National Institutes of Health.

References

1. Epstein EH. Basal cell carcinomas: attack of the hedgehog. Nat Rev Cancer. 2008; 8(10):743–754. [PubMed: 18813320]
2. Stacey SN, et al. New common variants affecting susceptibility to basal cell carcinoma. Nat Genet. 2009; 41(8):909–914. [PubMed: 19578363]
3. Markey AC, Lane EB, Macdonald DM, Leigh IM. Keratin expression in basal cell carcinomas. Br J Dermatol. 1992; 126(2):154–160. [PubMed: 1371396]
4. Yu M, et al. Superficial, nodular, and morpheiform basal-cell carcinomas exhibit distinct gene expression profiles. J Invest Dermatol. 2008; 128(7):1797–1805. [PubMed: 18200053]
5. Larouche D, Tong X, Fradette J, Coulombe PA, Germain L. Vibrissa hair bulge houses two populations of skin epithelial stem cells distinct by their keratin profile. FASEB J. 2008; 22(5): 1404–1415. [PubMed: 18162489]
6. Grachtchouk M, et al. Basal cell carcinomas in mice overexpressing Gli2 in skin. Nat Genet. 2000; 24(3):216–217. [PubMed: 10700170]
7. Grachtchouk V, et al. The magnitude of hedgehog signaling activity defines skin tumor phenotype. EMBO J. 2003; 22(11):2741–2751. [PubMed: 12773389]
8. Jih D, Shapiro M, James WD, Levin M, Gelfand J, Williams PT, Oakley RJ, Farkazadeh S, Seykora JT. Familial basaloid follicular hamartoma: lesional characterization and review of the literature. Am J Dermatopathol. 2003; 25:130–137. [PubMed: 12652194]
9. Callahan CA, et al. MIM/BEG4, a Sonic hedgehog-responsive gene that potentiates Gli-dependent transcription. Genes Dev. 2004; 18(22):2724–2729. [PubMed: 15545630]

10. McGowan KM, et al. Keratin 17 null mice exhibit age- and strain-dependent alopecia. Genes Dev. 2002; 16(11):1412–1422. [PubMed: 12050118]
11. Kerns ML, DePianto D, Dinkova-Kostova AT, Talalay P, Coulombe PA. Reprogramming of keratin biosynthesis by sulforaphane restores skin integrity in epidermolysis bullosa simplex. Proc Natl Acad Sci U S A. 2007; 104(36):14460–14465. [PubMed: 17724334]
12. Cataisson C, et al. Inducible cutaneous inflammation reveals a protumorigenic role for keratinocyte CXCR2 in skin carcinogenesis. Cancer Res. 2009; 69(1):319–328. [PubMed: 19118017]
13. Elias PM, Schmuth M. Abnormal skin barrier in the etiopathogenesis of atopic dermatitis. Curr Opin Allergy Clin Immunol. 2009; 9(5):437–446. [PubMed: 19550302]
14. Demehri S, Morimoto M, Holtzman MJ, Kopan R. Skin-derived TSLP triggers progression from epidermal-barrier defects to asthma. PLoS Biol. 2009; 7(5):e1000067. [PubMed: 19557146]
15. Bradley PP, Priebat DA, Christensen RD, Rothstein G. Measurement of cutaneous inflammation: estimation of neutrophil content with an enzyme marker. J Invest Dermatol. 1982; 78(3):206–209. [PubMed: 6276474]
16. Hardman MJ, Sisi P, Banbury DN, Byrne C. Patterned acquisition of skin barrier function during development. Development. 1998; 125(8):1541–1552. [PubMed: 9502735]
17. Berger A. Th1 and Th2 responses: what are they? BMJ. 2000; 321(7258):424. [PubMed: 10938051]
18. Steinman L. A brief history of T(H)17, the first major revision in the T(H)1/T(H)2 hypothesis of T cell-mediated tissue damage. Nat Med. 2007; 13(2):139–145. [PubMed: 17290272]
19. Nickoloff BJ. Cracking the cytokine code in psoriasis. Nat Med. 2007; 13(3):242–244. [PubMed: 17342112]
20. Phillips WG, Feldmann M, Breathnach SM, Brennan FM. Modulation of the IL-1 cytokine network in keratinocytes by intracellular IL-1 alpha and IL-1 receptor antagonist. Clin Exp Immunol. 1995; 101(1):177–182. [PubMed: 7621586]
21. Lund SA, Giachelli CM, Scatena M. The role of osteopontin in inflammatory processes. J Cell Commun Signal. 2009
22. Jee SH, et al. Interleukin-6 induced basic fibroblast growth factor-dependent angiogenesis in basal cell carcinoma cell line via JAK/STAT3 and PI3-kinase/Akt pathways. J Invest Dermatol. 2004; 123(6):1169–1175. [PubMed: 15610530]
23. Hattori Y, et al. Vascular expression of matrix metalloproteinase-13 (collagenase-3) in basal cell carcinoma. Exp Mol Pathol. 2003; 74(3):230–237. [PubMed: 12782009]
24. Ying S, et al. C-C chemokines in allergen-induced late-phase cutaneous responses in atopic subjects: association of eotaxin with early 6-hour eosinophils, and of eotaxin-2 and monocyte chemoattractant protein-4 with the later 24-hour tissue eosinophilia, and relationship to basophils and other C-C chemokines (monocyte chemoattractant protein-3 and RANTES). J Immunol. 1999; 163(7):3976–3984. [PubMed: 10491000]
25. Yuspa SH. The pathogenesis of squamous cell cancer: lessons learned from studies of skin carcinogenesis--thirty-third G. H. A. Clowes Memorial Award Lecture. Cancer Res. 1994; 54(5): 1178–1189. [PubMed: 8118803]
26. Eckert RL, et al. S100 proteins in the epidermis. J Invest Dermatol. 2004; 123(1):23–33. [PubMed: 15191538]
27. Braff MH, Bardan A, Nizet V, Gallo RL. Cutaneous defense mechanisms by antimicrobial peptides. J Invest Dermatol. 2005; 125(1):9–13. [PubMed: 15982297]
28. Miyazaki H, et al. Down-regulation of CXCL5 inhibits squamous carcinogenesis. Cancer Res. 2006; 66(8):4279–4284. [PubMed: 16618752]
29. Lo BKYM, Zloty D, Cowan B, Shapiro J, McElwee KJ. CXCR3/ligands are significantly involved in the tumorigenesis of basal cell carcinoma. Am J Pathol. 2010; 176(5):2435–2446. [PubMed: 20228225]
30. Pasparakis M. Regulation of tissue homeostasis by NF-kappaB signalling: implications for inflammatory diseases. Nat Rev Immunol. 2009; 9(11):778–788. [PubMed: 19855404]
31. Tensen CP, et al. Genomic organization, sequence and transcriptional regulation of the human CXCL 11(1) gene. Biochim Biophys Acta. 1999; 1446(1–2):167–172. [PubMed: 10395932]

32. Smith JB, et al. Cloning and genomic localization of the murine LPS-induced CXC chemokine (LIX) gene, Scyb5. Immunogenetics. 2002; 54(8):599–603. [PubMed: 12439624]
33. Bunting K, et al. Genome-wide analysis of gene expression in T cells to identify targets of the NF-kappa B transcription factor c-Rel. J Immunol. 2007; 178(11):7097–7109. [PubMed: 17513759]
34. Tong X, Coulombe PA. Keratin 17 modulates hair follicle cycling in a TNFalpha-dependent fashion. Genes Dev. 2006; 20(10):1353–1364. [PubMed: 16702408]
35. Kim S, Wong P, Coulombe PA. A keratin cytoskeletal protein regulates protein synthesis and epithelial cell growth. Nature. 2006; 441(7091):362–365. [PubMed: 16710422]
36. van de Rijn M, et al. Expression of cytokeratins 17 and 5 identifies a group of breast carcinomas with poor clinical outcome. Am J Pathol. 2002; 161(6):1991–1996. [PubMed: 12466114]
37. Sarbia M, et al. Differentiation between pancreaticobiliary and upper gastrointestinal adenocarcinomas: is analysis of cytokeratin 17 expression helpful? Am J Clin Pathol. 2007; 128(2):255–259. [PubMed: 17638659]
38. Paus R, Ito N, Takigawa M, Ito T. The hair follicle and immune privilege. J Investig Dermatol Symp Proc. 2003; 8(2):188–194.
39. McGowan KM, Coulombe PA. Onset of keratin 17 expression coincides with the definition of major epithelial lineages during skin development. J Cell Biol. 1998; 143(2):469–486. [PubMed: 9786956]
40. Bernot KM, Coulombe PA, McGowan KM. Keratin 16 expression defines a subset of epithelial cells during skin morphogenesis and the hair cycle. J Invest Dermatol. 2002; 119(5):1137–1149. [PubMed: 12445204]
41. Bernot KM, Coulombe PA, Wong P. Skin: an ideal model system to study keratin genes and proteins. Methods Cell Biol. 2004; 78:453–487. [PubMed: 15646628]

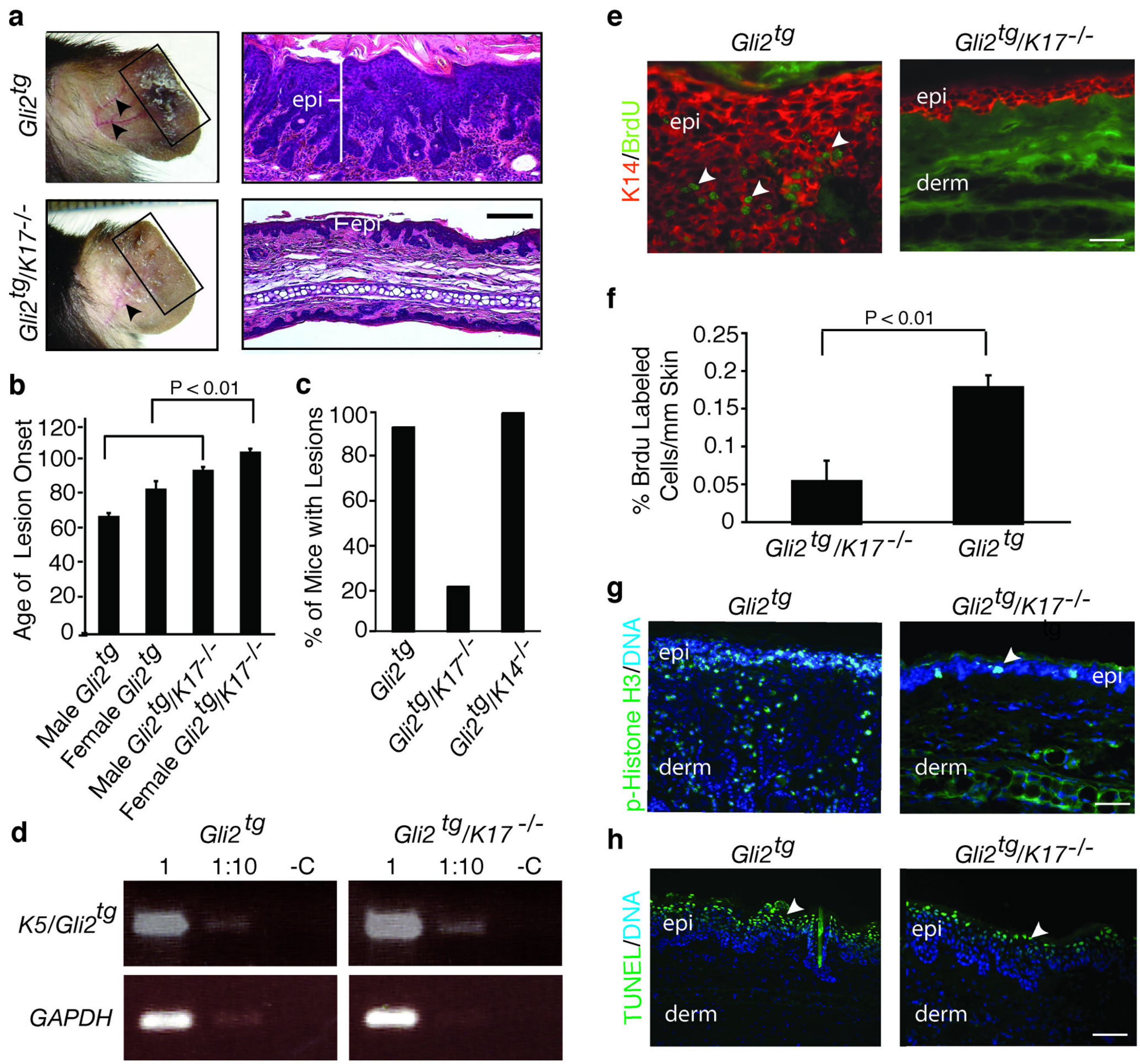

Figure 1.

Absence of K17 delays the onset of ear lesions, and epidermal hyperplasia, in *Gli2^tg^* mice. (a) Age-matched P80 *Gli2^tg^* and *Gli2^tg^/K17^−/−^* male mice. Left, pictures of intact ear. Box highlights lesional tissue in *Gli2^tg^* mice. Arrows point to blood vessels, prominent in *Gli2^tg^* mice. Right, hematoxylin-eosin stained ear tissue section, showing expansion of epidermis (epi). (b), Mean age (± s.e.m.) of onset of macroscopic ear lesions in *Gli2^tg^* and *Gli2^tg^/K17^−/−^* mice, stratified by gender. (c) Percentage of mice with ear lesions at P80 in the *Gli2^tg^*, *Gli2^tg^/K17^−/−^*, and *Gli2^tg^/K14^−/−^* strains of mice. (d) RT-PCR assay of levels of Gli2 transgene expression in *Gli2^tg^* and *Gli2^tg^/K17^−/−^* mice (GAPDH: loading control). (e) Immunostaining for BrdU in ear tissue of P80 male *Gli2^tg^* and *Gli2^tg^/K17^−/−^* mice.epi, epidermis; derm, dermis. (f) Quantitation of BrdU-positive keratinocytes/mm of epidermis seen in (e). (g, h) Immunostaining for phospho-Histone H3 (g), marking mitotic activity, and TUNEL staining (h), detecting apoptotic cells, in P80 male *Gli2*^{tg} and *Gli2*^{tg}*/K17*$^{-/-}$. Scale bars: a (50μm), e,g,h (20μm).

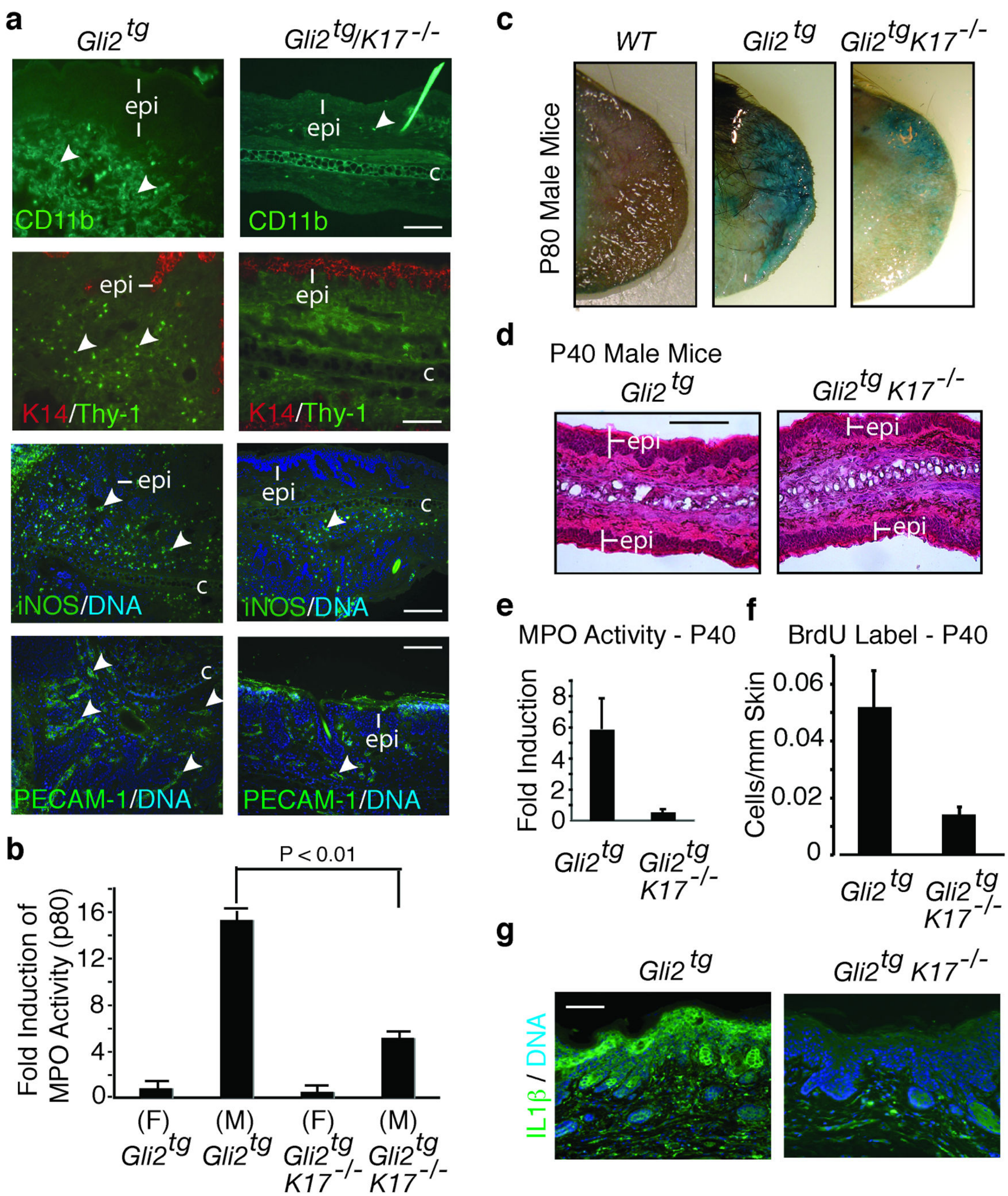

Figure 2.

Role of inflammation in the onset of ear lesions. (a) Immunodetection of infiltrating immune cells and vasculature in *Gli2*^{tg} and *Gli2*^{tg}*/K17*$^{-/-}$ male mice at P80 using antibodies to CD11b, Thy-1, iNOS, and PECAM-1 (see arrows). Labeling key provided in lower left corner. (b) Quantification of myeloperoxidase activity (MPO; mean ± s.e.m.) in ear tissue of mice at P80, normalized to female *Gli2*^{tg} mice. (c) In situ beta-galactosidase staining in P80 male ear tissue of various genotypes. Blue staining reflects loss of barrier integrity. (d) Hematoxylin-eosin stained ear tissue of male mice at P40. (e) Myeloperoxidase activity in ear tissue of P40 male mice, normalized to female *Gli2*^{tg} (mean ± s.e.m.). (f) Quantification of BrdU labeled cells/um of epidermis in P40 male mice. (g) Immunostaining for IL-1β in the epidermis (epi) of P80 male ear tissue. Scale bars: a (20μm), c (25μm), d (50μm).

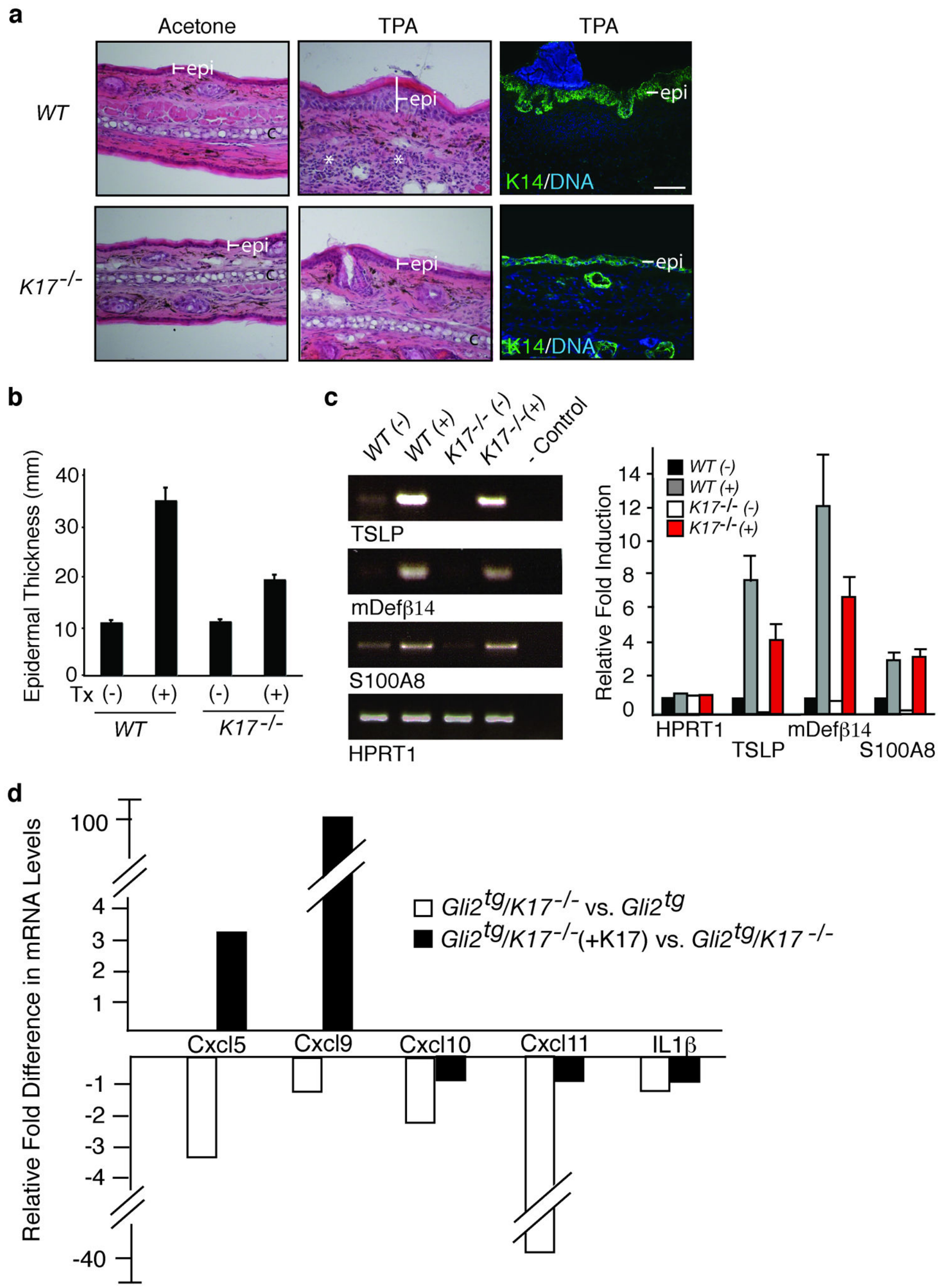

Figure 3.

Absence of K17 blunts epidermal hyperplasia and alters inflammation in a chemical model of dermatitis. *Wildtype* and *K17*$^{-/-}$ mouse ears were treated with acetone (vehicle control) or TPA. (a) Hematoxylin-eosin stained tissue sections depicting the effect of TPA treatment on thickness of epidermis. Right panel: Expansion of basal layer visualized by immunostaining for K14. Scale bars: 20 μm. (b) Epidermal thickness (mean ± s.e.m.), as conveyed by K14 staining, in vehicle (−) and TPA-treated (+) male mouse ears. (c) Right: Semi-quantitative RT-PCR survey of targets associated with loss of barrier integrity. Left:

Quantitation of RT-PCR results shown in c. (d) Cytokine/chemokine expression in primary cultures of *Gli2*^{tg} and *Gli2*^{tg}*/K17*$^{-/-}$ keratinocytes 12 hours after TPA. For d and e, fold change represents changes due to loss of K17 (compilation of 3 assays involving distinct pools of mRNAs). (f) Changes in cytokine and chemokine expression in *Gli2*^{tg}*/K17*$^{-/-}$ after reintroduction of K17 via transfection (triplicate).

Table 1

Comparing the inflammatory and immune response in ear lesions, in male *Gli2*^{tg}/*K17*$^{-/-}$ relative to male *Gli2*^{tg} mice, at P80 and P40. The fold change reported represents alterations in mRNA levels due to loss of *K17*. Values reflect compiled data from three experiments involving distinct pools of cDNAs.

Postnatal day 80		
Cytokine/Chemokine (Th1)	**Fold Change**	**P-Value**
Spp1	−14.83	0.013
Ccl3	−14.80	0.003
Cxcl5	−10.56	0.007
IL1β	−10.20	0.009
Ccl4	−8.78	0.016
Ccr1	−4.92	0.014
Cxcr2	−3.53	0.051
Ccr5	−2.53	0.054
Cxcl10	−1.73	0.036
Ccl5	−1.69	0.022
TNFα	−1.18	0.076
IFNγ	1.31	0.440
Cytokine/Chemokine (Th2)	**Fold Change**	**P-Value**
Ccl24	8.85	0.008
Ccl17	4.21	0.000
Ccr4	3.24	0.004
Ccl22	3.09	0.007
Ccl1	2.97	0.003
Ccl11	2.17	0.046
IL13	2.11	0,004
IL15	1.62	0.059
IL4	1.20	0.100
IL20	−1.06	0.900
Cytokine/Chemokine (Th17)	**Fold Change**	**P-Value**
Mmp13	−25.06	0.001
Csf3	−19.57	0.003
IL6	−17.12	0.001
Cxcl2	−9.99	0.017
Cxcl5	−9.37	0.001
Cxcl1	−6.52	0.002
Syk	−6.46	0.043
Mmp9	−5.62	0.004
Clec7a	−4.66	0.005
Mmp3	−2.67	0.023
IL10	−2.46	0.005

Postnatal day 80		
Cd3g	4.51	0.069
IL25	4.01	0.048
Cd3d	3.56	0.021
IL5	2.51	0.012
IL15	1.63	0.035
Postnatal day 40		
Cytokine/Chemokine (Th1)	**Fold Change**	**P-Value**
IL1β	−4.21	0.028
Cxcl5	−3.52	0.005
Ccr1	−2.96	0.001
Cxcr2	−1.98	0.019
Ccl3	−1.51	0.233
Cytokine/Chemokine (Th2)	**Fold Change**	**0.014**
IL20	12.66	0.090
IL4	5.24	0.121
IL13	5.03	0.110
Ccl24	1.59	0.258
Ccl17	1.11	0.076

Table 2

Comparing the inflammatory and immune response in TPA-treated ear tissue from *K17*$^{-/-}$ and wildtype mice. The fold change reported represents alterations in mRNA levels due to loss of *K17*. Values reflect compiled data from three experiments involving distinct pools of cDNAs.

Cytokine/Chemokine (Th1)	**Fold Change**	**P-Value**
Ccl3	−2.97	0.001
Cxcl5	−2.44	0.002
Cxcl1	−1.90	0.244
Ccl4	−1.86	0.009
IL1β	−1.70	0.010
Cxcl9	−1.20	0.070
IFNγ	1.48	0.355
Cytokine/Chemokine (Th2)	**Fold Change**	**P-Value**
IL20	7.10	0.003
Ccl22	1.88	0.004
IL15	1.40	0.001
IL4	1.20	0.100
IL10	1.11	0.356